Faint Companion Search to O-stars using the Adaptive Optics System on the 3.63-meter Telescope on Haleakala[*]

Nils Turner[a], Theo ten Brummelaar[a], Lewis Roberts[b]

[a]Georgia State University, c/o Mount Wilson Observatory,
Mount Wilson CA 91023
[b]The Boeing Company, 535 Lipoa Pkwy, Suite 200, Kihei HI 96753

ABSTRACT

We present results of our survey of faint companions to O-stars using the adaptive optics (AO) system on the 3.63-meter Advanced Electro-Optical System (AEOS) telescope at the summit of Haleakala, on the island of Maui. The AEOS telescope is part of the United States Air Force's Maui Space Surveillance Site.

We have surveyed most of the O-stars brighter than V magnitude 8.0 in the declination range of -25 to +65 degrees for faint companions. We are using the I-band (800 nm central wavelength, 150 nm approximate FWHM) for the survey. This is done for two reasons: 1) the distinctly red filter will de-emphasize the O-star primary and enhance the faint (presumably redder) secondary, increasing the dynamic range; and 2) using I-band allows all of the shorter wavelength light to be sent to the AO system, increasing its performance for fainter stars. We describe the scientific results of our survey as well as the reduction process we used to generate relative photometric results from a 12-bit frame transfer camera with no native ability to generate a bias frame.

Keywords: binaries: general – binaries: visual – instrumentation: adaptive optics

1. INTRODUCTION

We have performed most of a multiplicity survey of O stars obtainable by the AEOS telescope, both brightness- and declination-wise. Previous multiplicity surveys of these hot stars have been done using speckle interferometry[1] or spectroscopy and so have been biased towards systems with relatively small brightness ratios. The high resolution and dynamic range of AO observations in combination with observations in the *I* band will greatly increase the number of faint and cooler companions that can be detected. Future follow-up programs and a more in-depth analysis of the negative detections listed in Section 3.1 can increase the scope of the findings in Ref. 1 (Mason *et al.*, 1998).

2. OBSERVATIONS

2.1. The AEOS AO System

The AO system of the AEOS 3.63-meter telescope is described in detail elsewhere.[2–5] In short, the telescope (an altitude-azimuth design) uses a standard 7 mirror configuration (the optical axis between mirrors 3 and 4 is along the altitude mechanical axis; the optical axis between mirrors 6 and 7 is along the azimuth mechanical axis) to convey light to the AO system located several floors below the telescope. The AO system can send the compensated beam to one of seven experiment rooms. In its standard configuration, all light shorter than

---

0.7 μm in wavelength is used for tip/tilt and wavefront detection/correction. Longer wavelengths are available for science.

The system features a Shack-Hartmann wavefront sensor driving an Xinetics 941-actuator deformable mirror. The heart of the wavefront sensor is a 128×128 pixel low-noise CCD, capable of a 2.5 kHz frame rate. Wavefront reconstruction is accomplished through a modified least-squares reconstructor.

2.2. Observing Strategy

The camera used for this work is the standard visible imager (VisIm) of the AEOS telescope. The camera is a Pentamax 512×512 pixel CCD cooled detector array. The maximum frame rate is slightly greater than 4 Hz. The spectral range is 0.7 to 1.1 μm. The field of view can be remotely selected, from a choice of 51.6, 120, or 300 μrad. Because the primary mission of the AEOS telescope is satellite imagery, the VisIm camera was designed to that end, making it less than optimal for astronomical objects. For speed of readout, the camera uses frame transfer technology and a 12-bit digitizer. Frame transfer cameras have a higher readout noise than the typical camera used in astronomy. For bright objects, the 12-bit digitizer well can quickly fill up. Because of this, neutral density filters are integral to operations. Finally, the VisIm is not equipped with a shutter.

In light of these limitations, we developed an observing strategy to cope. Because all light blueward of 700 nm is used for making the AO system work, one wants to avoid target objects that emit most of their light towards the red end of the spectrum. This led to the choice of O stars as the primary target objects. To match much of the visible AO science published in the literature, we use the Bessel I filter[6] for the science band. As an added benefit, the I band will de-ephemsize the bluish O-star primary to a certain extent, perhaps allowing a fainter companion to be seen than would be allowed with a shorter wavelength filter.

To deal with the higher readout noise and 12-bit digital signal well, many frames are taken at a short enough exposure time to avoid overflowing the digitizer (keeping the counts below 4096). In practice, we have found that 250 to 1000 frames (depending on the ultimate noise floor desired) is adequate (see Section 2.5). While that number of frames is 5 to 20 times more than is normally required, the system has no problem keeping up with the data flow, and in this day and age, data space is inexpensive.

Finally, the lack of a mechanical shutter on the VisIm system affects only data taken on brighter stars. This "smears" the star a small bit in the direction of the frame transfer, effectively creating a higher noise floor in one direction away from the target star. If there were a faint companion in that direction from the star (as opposed to another one), it would have to be brighter to be detected. For the dimmer stars, the amount of stellar exposure to the camera during the frame transfer is undetectable.

2.3. Observing List

Though the AEOS telescope AO system is capable of observing down to an elevation of -5°, experience has shown that AO systems perform best at elevations higher than 45°. This information, along with the latitude of the telescope (20°42'30.5"), provides the basis for the primary star list: O-stars between the declination angles of -25° and +66°, brighter than m$_V$=8.0. This list has 90 members. To increase the number of objects, the primary star list was supplemented by a secondary list: O-stars between the declination angles of -45° and +86°, brighter than m$_V$=8.0, and not in the primary list. This list has 41 members.

2.4. Data Reduction and Calibration

The traditional way to get a bias frame is to close the shutter, clear the detector, and immediately read the detector out. The VisIm camera is constantly reading out the data. In the finite period of time it takes to read the frame out, the camera is effectively taking a dark frame, albeit a short one. The minimum exposure time is 10 milliseconds. For many of the objects, that is too long compared to the total exposure time to give accurate debiasing.

To get a bias frame, a sequence of dark frames of ever longer exposure times is taken. The longest exposure time is usually similar in length to the longest exposure time expected to be taken during the course of observation (usually about 3 seconds). A pixel-by-pixel least squares analysis is done on the sequence of dark frames. The 2-dimensional array of "slopes" gives the dark frame, while the "intercepts" give the bias frame.

In reducing the data, all images were debiased and flatfielded in the conventional way. For the sequence of images, a weighted shift-and-add was used to create the final image. The weighted shift-and-add algorithm[7] is a modification of the traditional image stacking algorithm which takes the AO performance (usually correlated with seeing conditions, but not always) in each individual frame into account. The frames with higher peak values (which represent better AO performance) influence the final image more than frames with lower peak values. The fitting algorithm is described in detail in Ref. 8 (ten Brummelaar *et al.*, 2000). In short, the point spread function (PSF) used to represent the system performance is the primary star in the image with a few modifications; near the primary, the PSF is a pixel-for-pixel table of numbers, while farther out, the PSF is a radially symmetric series of values. This PSF is fitted to the primary and secondary components and iterated upon until the intensity ratio converges. The algorithm outputs the x- and y-values of the primary and secondary and a magnitude difference.

The VisIm camera is equipped with a rotating dove prism to compensate for the image rotation inherent in an altitude-azimuth telescope. When the derotator is set to "astronomical mode", north is at the top of the frame. The image-scale calibration was done by taking data on several known binary stars[†], calculating the position angle and separation at the time the data were taken (using the known orbital elements), and comparing it to the x- and y-values of the primary and secondary positions measured from the data.

2.5. Sensitivity Issues

No AO system performs perfect wavefront reconstruction. The net effect of this imperfect wavefront reconstruction is to create an image with a peak value about 20% of what it could be, on top of a slightly raised halo. The halo is the residual light that did not make it into the image peak and continues a long way out from the image peak. In addition, AO systems employing the Fried geometry within their wavefront sensors (a common geometry used with Shack-Hartmann wavefront sensors) leave an additional residual "waffle pattern". All of these effects conspire to make the detection of faint companions a function of distance from the primary as well as magnitude difference.

Figure 1 shows a "typical" radial profile reworked to show the primary/faint-companion magnitude difference (at *I* band) potentially detectable as a function of radius from the primary. The curves are (from the bottom) the detectability for 1, 10, 50, 100, 250, and 1000 co-added frames. Notice the "shoulder" at about 1 arcsec radius in the diagram. This is a consequence of the "waffle pattern" referred to earlier. Typically, for Fried geometry wavefront sensors, there are four raised spots centered around the primary. These four spots are averaged over the annulus to produce the shoulder in figure 1. The slope upward towards larger radii is due to the decreasing effect of the AO halo.

Keep in mind that figure 1 is only a "rule-of-thumb" relation. AO systems are sensitive to raw seeing conditions, apparent brightness of the primary object, and optical alignment. As a result, depending on conditions, a faint companion right near the threshold of detection might be detectable under relatively good atmospheric conditions, but be lost under poorer conditions. Also, for primary stars near the overall correction magnitude limit for the AEOS AO system will not have as good a wavefront correction and therefore may not concentrate the light of the faint companion enough to be detected above the background noise.

3. RESULTS

Determination of whether a reduced data set (bias/dark/flat adjusted and shift-and-added) contains a companion or not is determined manually. We have found that the human eye (with its attached brain) is the best way to determine whether a bump in the background is a flat-fielding error, a noise spike, a dust mote, or a faint companion. A further check to this manual determination is done by the PSF fitting routine. If the faint companion profile does not have a plausible match to the PSF (that is to say that its profile is a noise spike

---

[†]The U. S. Naval Observatory maintains the *Sixth Catalog of Orbits of Visual Binary Stars*, a catalog of binary stars with known orbital elements. In addition, they maintain a subset of that catalog, the "Calibration Candidates" list – a selection of systems with higher quality orbital elements or wider systems with lower quality orbital elements, but with a long enough period that the predicted positions will be quite accurate for years to come. It is available on the World Wide Web at http://ad.usno.navy.mil/wds/orb6.html.
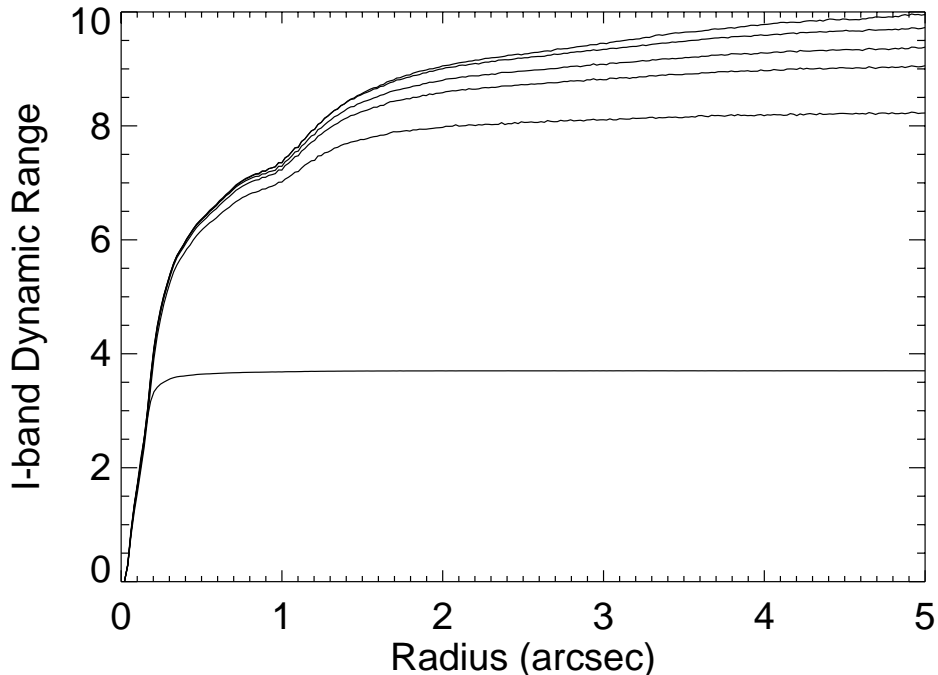
Figure 1. Primary/Secondary magnitude difference as a function of radius. Bottom to top, these curves represent this relation for data from 1, 10, 50, 100, 250, and 1000 frames. The dynamic range scale on the y-axis is based on the peak count in each frame being 3500 counts. The dynamic range improves the closer one gets to the saturation value of 4095 counts.

or broadish flat-field error), the fitting routine will usually fail. With this in mind, the companions detected in this way (and "verified" by the PSF fitting routine) may still be spurious detections.

3.1. Stars with No Detected Companions

Table 1 lists all the "no companion" detections so far of the objects on the O stars list. The data were taken under very different seeing conditions, so a negative result does not necessarily mean that there was no companion, just that any companion that might be there will be close to the thresholds defined by figure 1. Note also that this survey only samples the field within a 5 arcsecond radius of the primary object.

3.2. Stars with Detected Companions

Table 2, lists all the positive companion detections, both previously known and newly discovered (flagged with an asterisk, "*"). If a Washington Double Star (WDS) system designation is available, it is listed in the table as well. In the following subsections, we discuss each new discovery in turn.

3.2.1. HD 15558 = WDS 02327+6127

The companion is only marginally visible above the background. Due to its extreme faintness and reasonably large separation from the primary, it could either be a spurious detection or a background star. The WDS lists only one companion to this star, a companion at a separation of about 9 seconds of arc and about 2 magnitudes fainter. The new discovery does not match that companion.

Object	Date	Object	Date	Object	Date
HD 108	2001.74504	HD 149757	2002.22428	HD 186980	2001.73660
HD 1337	2001.73412	HD 152003	2001.38928	HD 188001	2001.73377
HD 14633	2001.74509	HD 152235	2001.38930		2001.74471
HD 14947	2001.74548	HD 152314	2001.40290	HD 190864	2001.73646
HD 18326	2001.74513	HD 154450	2001.40300	HD 191612	2001.73649
HD 19820	2001.74516		2001.49569	HD 192281	2001.73652
03243+4952	2001.73421	HD 157857	2002.23828	HD 192639	2001.73657
HD 24912	2001.73423	HD 158902	2001.46863	HD 193443	2001.73663
HD 37043	2001.74554	HD 162978	2001.74461	HD 199579	2001.73379
HD 39680	2002.24035	HD 163800	2001.49598	HD 201345	2001.73670
HD 41161	2001.86590		2001.51754	HD 203064	2001.73370
HD 42088	2001.86593	HD 163758	2001.49601		2001.73415
HD 45314	2001.09886		2001.51790		2001.74475
HD 46149	2001.86602	HD 164637	2001.51793	21395+4144	2001.73385
HD 46223	2001.86611	HD 164816	2001.67093	HD 207198	2001.73634
HD 46966	2002.23763	HD 164906	2001.67101	HD 209481	2001.73408
HD 48099	2002.24045	HD 165052	2001.67105	HD 209975	2001.73672
HD 52266	2001.97537	HD 165319	2001.67109	HD 210839	2001.73417
HD 54662	2002.02180	HD 165516	2001.67113	HD 210809	2001.73685
	2002.24041	HD 167971	2001.74464	HD 214680	2001.73387
HD 57682	2001.92893	HD 169454	2001.67116		2001.73691
HD 60848	2001.09897		2001.73639	HD 216898	2001.74506
HD 93521	2001.09917	HD 170938	2001.67119		
HD 148688	2001.38914		2001.73644		
HD 149404	2001.38924	HD 175876	2001.74467		

Table 1. Table of negative results and the date at which no companion was detected.

3.2.2. HD 17505 = WDS 02511+6025

The profile of the image matches the profile of the primary quite well, so the new discovery is definitely stellar in nature. The distances of the new discovery and the closest companion (see the next paragraph) are too much alike to make this new companion a likely dynamic member of the system. It is most likely a background star. The WDS lists 6 companions to this star, the closest at a separation of about 2 seconds of arc, and the farthest about 125 seconds of arc. The 2-second companion is visible in the image and is listed in Table 2. The new detection is a little bit further out in radius.

3.2.3. HD 47129

The new discovery is definitely stellar in nature. Its profile also matches the primary quite well. The differential magnitude explains why speckle interferometry did not detect it. The relatively small separation explains why wide-field surveys did not detect it. The WDS lists no companions to this star.

3.2.4. HD 164863 = WDS 18042-2230

The new discovery is definitely stellar in nature. Its profile also matches the primary quite well. The differential magnitude explains why speckle interferometry did not detect it. The relatively small separation explains why wide-field surveys did not detect it. The WDS lists only one companion to this star, a companion at a separation of about 30 seconds of arc and about 1.5 magnitudes fainter. The new discovery does not match that companion.

3.2.5. HD 193514

The new discovery is definitely stellar in nature. Its profile also matches the primary quite well. It is not understood why this star was missed by wide-field surveys. The WDS lists no companions to this star.

Object	Date	Sep. (")	Δm_I	WDS	New Disc.
HD 15558	2001.74498	4.534	7.30	02327+6127	*
HD 17505	2001.74501	2.162	1.66	02511+6025 AB	
	2001.74501	4.690	6.89	02511+6025	*
HD 24431	2001.74545	0.736	2.90	03556+5238	
HD 36861	2001.74283	4.345	1.96	05351+0956 AB	
	2001.74559	4.297	2.17	05351+0956 AB	
HD 37022	2001.74563	4.256	4.94	05353-0523	
05387-0236	2001.74561	0.244	1.32	05387-0236 AB	
HD 37742	2001.74552	2.415	2.37	05407-0157 Aa-B	
HD 46150	2001.09893	3.598	4.88	06319+0457 AB	
HD 47129	2002.24043	1.204	5.14		*
HD 47839	2001.74565	2.956	3.17	06410+0954 Aa-B	
HD 152408	2001.40296	5.505	5.69	16550-4109	
HD 157038	2001.46861	2.795	6.64	17227-3748 AB	
HD 164863	2001.67099	0.483	4.89	18042-2230	*
HD 190429	2001.73374	1.972	0.73	20035+3601 Aa-B	
HD 193322	2001.66832	2.740	2.40	20181+4044 Aa-B	
	2001.73641	2.753	2.13	20181+4044 Aa-B	
HD 193514	2001.73666	4.852	5.85		*
HD 206267	2001.73382	1.817	5.66	21390+5729 AB	
HD 217086	2001.73688	2.851	3.41	22568+6244	
	2001.73688	3.243	7.73	22568+6244	*

Table 2. Table of positive results (results for which at least one companion was found). The first column is the HD number (if available, otherwise, the IAU coarse coordinates), the second the date, the third the separation in seconds of arc, the fourth the differential magnitude at *I*, the fifth the Washington Double Star system designation (if available), and the sixth a new discovery flag.

3.2.6. HD 217086 = WDS 22568+6244

The profile of the image matches the profile of the primary quite well, so the new discovery is definitely stellar in nature. The distances of the new discovery and the known companion (see the next paragraph) are too much alike to make this new companion a likely dynamic member of the system. It is most likely a background star. The WDS lists only one companion to this star, a companion at a separation of about 3 seconds of arc and about 3.5 magnitudes fainter. This companion is visible in the image and is listed in Table 2.

4. CONCLUSION

In our (nearly completed) survey of O stars, we have 3 definite new companion detections, 2 detections that are likely to be background stars, and one that may be just a noise detection, but might turn out to be a star afterall. More data needs to be collected to verify or disprove the the existence of the marginal detections. To date we have looked at 81 of 90 stars in the primary list, and 11 of 41 stars in the secondary list. More work is needed to determine the nature of the new detections, multi-color differential magnitudes and spectroscopic information most importantly.

ACKNOWLEDGMENTS

REFERENCES

1. B. D. Mason, D. R. Gies, W. I. Hartkopf, W. G. Bagnuolo, Jr., T. ten Brummelaar, and H. A. McAlister, "ICCD speckle observations of binary stars. XIX. - an astrometric/spectroscopic survey of O stars," *A.J.* **115**, pp. 821–847, 1998.

2. R. Abreu, S. N. Gullapalli, W. M. Rappoport, R. Pringle, and W. P. Zmek, "Performance evaluation of the SAAO adaptive optics system," in *Proceedings of the SPIE*, S. Basu, S. J. Davis, and E. A. Dorko, eds., **3931**, pp. 300–310, SPIE – The International Society for Optical Engineering, (PO Box 10, Bellingham, Washington 98227-0010 USA), 2000. Gas, Chemical, and Electrical Lasers and Intense Beam Control and Applications.

3. R. Abreu, D. P. Chadwick, R. D'Amico, C. D. Delp, S. N. Gullapalli, D. Hansen, M. Marchionna, M. E. Meline, W. M. Rappoport, L. Mendyk, R. Pringle, K.-L. Shu, W. Swanson, and W. P. Zmek, "SAAO adaptive optics system," in *Proceedings of the SPIE*, S. Basu, S. J. Davis, and E. A. Dorko, eds., **3931**, pp. 272–284, SPIE – The International Society for Optical Engineering, (PO Box 10, Bellingham, Washington 98227-0010 USA), 2000. Gas, Chemical, and Electrical Lasers and Intense Beam Control and Applications.

4. S. N. Gullapalli, R. Abreu, W. M. Rappoport, , W. P. Zmek, and R. Pringle, "Modeling of the SAAO adaptive optics system," in *Proceedings of the SPIE*, S. Basu, S. J. Davis, and E. A. Dorko, eds., **3931**, pp. 285–299, SPIE – The International Society for Optical Engineering, (PO Box 10, Bellingham, Washington 98227-0010 USA), 2000. Gas, Chemical, and Electrical Lasers and Intense Beam Control and Applications.

5. L. C. Roberts Jr. and C. R. Neyman, "Characterization of the AEOS adaptive optics system," *P.A.S.P.* , 2002. in press.

6. M. S. Bessel, "UBVRI passbands," *P.A.S.P.* **102**, pp. 1181–1199, 1990.

7. T. ten Brummelaar, W. I. Hartkopf, H. A. McAlister, B. D. Mason, L. C. Roberts, Jr., and N. H. Turner, "Scientific results using the Mount Wilson Institute adaptive optics system," in *Proceedings of the SPIE*, D. Bonaccini and R. K. Tyson, eds., **3353**, pp. 391–397, SPIE – The International Society for Optical Engineering, (PO Box 10, Bellingham, Washington 98227-0010 USA), 1998. Meeting held in Kona, Hawaii, 20–24 March 1998.

8. T. ten Brummelaar, B. D. Mason, H. A. McAlister, L. C. Roberts, Jr., N. H. Turner, W. I. Hartkopf, and W. G. Bagnuolo, Jr., "Binary star differential photometry using the adaptive optics system at Mount Wilson Observatory," *A.J.* **119**, pp. 2403–2414, 2000.